Gross and net production during the spring bloom along the Western Antarctic Peninsula

Johanna A.L. Goldman[1], Sven A. Kranz[1,4], Jodi N. Young[1], Philippe D. Tortell[2], Rachel H.R. Stanley[3], Michael L. Bender[1], Francois M.M. Morel[1].

Corresponding author: Johanna A.L. Goldman, email: johannag@princeton.edu, Phone: 609-258-2612

[1] Department of Geosciences, Princeton University, Princeton, NJ, 08544, USA

[2] Department of Earth, Ocean and Atmospheric Sciences, Dept. of Botany, University of British Columbia, Vancouver, BC, V6T 1Z4, Canada

[3] Department of Marine Chemistry and Geochemistry, Woods Hole Oceanographic Institution, Woods Hole, MA, USA

[4] Present address: Department of Earth, Ocean and Atmospheric Sciences, Florida State University, Tallahassee, FL, 32306, USA

Word count:

Total	6303
Introduction	730
Material and methods	1738
Results	2568
Discussion	1122
Acknowledgements	145

4 Figures (Figures 1 and 2 in colors)

Supporting information:

Word count: 1550

6 Figures, 3 Tables, 4 Notes

Summary

- This study explores some of the physiological mechanisms responsible for high productivity near the shelf in the Western Antarctic Peninsula despite a short growing season and cold temperature.
- We measured gross and net primary production at Palmer Station during the summer 2012/2013 via three different techniques: 1) incubation with $H_2{}^{18}O$; 2) incubation with $^{14}CO_2$; and 3) *in situ* measurements of O_2/Ar and triple oxygen isotope. Additional laboratory experiments were performed with the psychrophilic diatom *Fragilariopsis cylindrus.*
- During the spring bloom, which accounted for more than half of the seasonal gross production at Palmer Station, the ratio of net to gross production reached a maximum greater than ~60%, among the highest ever reported. The use of multiple-techniques showed that these high ratios resulted from low heterotrophic respiration and very low daylight autotrophic respiration. Laboratory experiments revealed a similar ratio of net to gross O_2 production in *F.cylindrus* and provided the first experimental evidence for an important level of cyclic electron flow (CEF) in this organism.
- The low ratio of community respiration to gross primary production observed during the bloom at Palmer Station may be characteristic of high latitude coastal ecosystems and partially supported by a very active CEF in psychrophilic phytoplankton.

Key words: cold adaptation, cyclic electron flow, *Fragilariopsis cylindrus*, gross production, net community production, respiration, Western Antarctic Peninsula.

Introduction

The Western Antarctic Peninsula (WAP) is among the most productive regions in the Southern Ocean (Arrigo *et al.*, 2008a; Arrigo *et al.*, 2008b), where spring phytoplankton blooms result in a large Net Community Production (NCP= photosynthesis minus respiration) supporting an abundant and diverse ecosystem (Ducklow *et al.*, 2007). Over the past several decades, the WAP has also experienced some of the most extreme atmospheric warming on the planet (IPCC, Parry (2007)) with a concomitant rise of more than 1°C in sea surface temperature since the 1950s (Meredith & King, 2005). Significant research to date has focused on determining the effects of rising temperature on the magnitude of the spring bloom (e.g. Montes-Hugo *et al.* (2009)) but there is limited understanding of the mechanisms that control the rates of carbon fixation and consumption in these waters.

Photochemical reactions are nearly temperature independent and phytoplankton have developed several adaptive mechanisms to mitigate the effect of low temperature on the photosynthetic electron transport chain (see reviews by Mock and Hoch (2005), Morgan-Kiss *et al.* (2006) and Dolhi *et al.* (2013)). As a result, the light reaction of photosynthesis is little affected by low temperature under nutrient replete conditions. For the dark reaction, the reduced catalytic rates of various enzymes in the Calvin cycle at cold temperature can be partially compensated by the increased solubility of CO_2 over O_2 in water, an efficient carbon concentrating mechanism (Kranz *et al.*, accepted), and an increase in the cellular concentration of key enzymes, including Ribulose-1,5-bisphosphate carboxylase oxygenase, Rubisco (Young *et al.*, accepted). In contrast, respiratory processes have been reported to be highly sensitive to the change in temperature. Large decreases in respiration rate with decreasing temperature have been shown in previous studies of individual phytoplankton and macro-algae (Staehr & Birkeland, 2006; Padilla-Gamino & Carpenter, 2007) as well as in

numerous ecosystems (Valentini *et al.*, 2000; Regaudie-de-Gioux & Duarte, 2012; Yvon-Durocher *et al.*, 2012). It is unclear why phytoplankton growing at a given growth rate would need less energy from respiration at low than at higher temperature. One possibility is that psychrophilic phytoplankton may take advantage of the maintenance of the high activity of their photosystems to generate ATP via the photosynthetic apparatus.

In this study we used three different techniques to study primary production and respiration in the WAP (LTER-station B, Palmer station, Latitude: -64.7795; Longitude: -64.0725, sampling depth: 10m, total depth ~70m; Fig. S1) during the austral summer of 2012/2013. Comparing the results of three techniques provides insights into some of the mechanisms that control the primary productivity in the WAP. Two of these techniques are bottle incubations that measure production from the light reaction of photosynthesis ($H_2{}^{18}O$ incubation) or the dark reaction of photosynthesis ($^{14}CO_2$ incubation). In addition, measurements of biologically-derived O_2 supersaturation as well as of the isotopic composition of the O_2 pool, from *in situ* sample collection, allowed us to derive time-integrated ratios of Net/Gross production (the "triple oxygen isotope technique"; Luz and Barkan (2000); Prokopenko *et al.* (2011); Juranek and Quay (2013)). To further explore the underlying physiological processes, laboratory experiments were conducted with the model psychrophilic diatom *Fragilariopsis cylindrus*, including measurements of net and gross photosynthesis, respiration and cyclic electron flow.

Materials and methods

Field sampling and incubation experiments.

Sampling took place twice weekly in the morning at LTER-station B (Latitude: -64.7795; Longitude: -64.0725; total depth ~70m). Water from 10m depth was collected (monsoon pump; Waterra WSP-SS-80-

NC) and dispensed into acid washed (10% HCl) containers, rinsed thoroughly with MilliQ and on site water, for transport back to the shore-based laboratories. Back at shore, all containers were kept in a cold room (2°C) until processing, which typically occurred within 1 -2 hours of sample collection. Incubation experiments (described below) were conducted on sub-samples placed in a flow-through seawater tank shaded with neutral density screening to reduce irradiance by 50% (*LEE* filters 209 0.3ND). A continuous flow of seawater pumped from the shore (10m depth) was used for temperature control.

Pigment measurements and identification*.*

A known volume of sample (0.2-1L) was collected in duplicate and filtered onto a glass fiber filter (Whatman GF/F, nominal pore size= 0.7µm). After overnight extraction in 90% acetone at -20°C, chlorophyll *a* (Chl *a*) concentration for each duplicate was determined with a fluorometer (Turner Designs 10-AU), measuring the un-acidified and acidified sample to correct for phaeopigments (Welschmeyer, 1994). For pigment identification (chlorophyll and carotenoids), one liter of seawater was filtered under low light onto a GF/F, wrapped in aluminum foil, flash frozen in liquid nitrogen and subsequently stored at -80°C. Phytoplankton species composition for the three major taxa (diatoms, *Phaeocystis*, and cryptophytes) was determined from the abundance of the pigments fucoxanthin, 19' hexanoyloxyfucoxanthin and alloxanthin (Everitt *et al.*, 1990; Arrigo *et al.*, 2000). Quantification of pigments was conducted using HPLC analysis at the Estuarine Ecology Lab (University of South Carolina) following the protocol described in Pinckney *et al.* (1998).

Seawater Hydrography and meteorological measurements.

The Palmer station Long Term Ecological Research (PAL-LTER) program conducted regular depth profiles of temperature and salinity at LTER-station B using a Seabird SBE 19plus Seacat Profiler. These depth profile (Fig. S2) measurements were made within 1 – 2 hours of our regular

sampling times. Seawater density (Fig. S3) was computed from salinity and temperature using the TEOS-10 seawater equation of state (http://www.teos-10.org/software.htm). Surface PAR levels (*i.e.* irradiance between 400 and 700 nm wavelength) were measured by the Palmer Station Terra Laboratory using a LI-COR LI-190SA quantum sensor. Wind-speed data were obtained from the meteorological sensors on top of the Palmer Station Terra Laboratory.

O_2 measurements.

Dissolved [O_2] was measured by Winkler titration. Seawater was collected with a Go-flo bottle and transferred directly to Winkler bottles, taking care to avoid bubbles and to seal samples and reagents with no headspace. Samples for each sampling day were taken in duplicate. Titrations were performed using an amperometric oxygen titrator designed by Dr. Chris Langdon (Langdon, 1984; Culberson & Huang, 1987).The instrumental precision of the measurements is ± 2 µmol L^{-1} but the average precision of the duplicate was ± 4 µmol L^{-1}.

$H^{18}O_2$ incubations.

Gas tight bottles (145 ml, Pyrex) were rinsed and filled with collected seawater from the carboys. One bottle was set aside for immediate transfer (initial sample) while two bottles were spiked with 125µL $H_2{}^{18}O$ (Medical Isotopes, 97.6%) for a final enrichment of 412.4‰. The two experimental bottles were incubated for 4 to 8 hours in the aquarium tank outside the station. For our laboratory experiments we followed the same procedure but duplicate bottles were taken for immediate transfer (initial samples) and duplicate bottles were incubated in an illuminated incubator (150 µE m^{-2} s^{-1}) at 0.5°C. The samples were subsequently transferred into custom-made 500mL flasks equipped with Louwers-Hapert valves (LH flask), that had been previously spiked with 100µL of saturated $HgCl_2$, dried, and evacuated (~1.5 mTorr= ~0.2Pa). The LH flasks were then analyzed back in the laboratory at Princeton within 6 months. Prior to analysis, the liquid phase was first

equilibrated, and then carefully drained. LH flasks were then put in a freezing bath and the gas in each flask transferred into a stainless steel tube kept in a liquid helium tank. Each tube was allowed to warm up for one hour before analysis in a Delta Plus XP mass spectrometer for dO_2/Ar, $d^{18}O$ and $d^{15}N$ (see Emerson *et al.* (1995)). The increase of $[^{18}O^{16}O]$ provides a measurement of Gross photosynthesis (GP) in the bottle, while the change in $[O_2]$ during the incubation provides the net production in the light in the bottle (NBP_L). The difference of the two gives respiration in the light in the bottle. The errors were calculated as standard deviation of the duplicates. The values were converted from oxygen evolution to carbon fixation using a photosynthetic quotient (PQ) based on C/N ratios from Young *et al.* (accepted) and derived from electrons balance:

PQ= $\frac{mol\ O_2}{mol\ C} = \frac{\frac{1}{4}mol\ e^-}{mol\ C} = 1 + 2 * \frac{N}{C}$. This equation assumes all nitrogen source is NO_3^- and an average photosynthetic product of $CH_{2+3N/C}\ ON_{N/C}$.

All the measurements and values used can be found in Table S1.

^{14}C incubations.

We used a ^{14}C-based incubation approach to measure C fixation rates by phytoplankton assemblages. Samples were incubated in polycarbonate bottles (125 ml), with varying amounts for $NaH^{14}CO_3$ in the flow-through seawater tank. Triplicate samples for Gross Primary Production (GPP) measurements were spiked with 10 µCi $H^{14}CO_3^-$ and incubated in the tank for 2h. Both incubations were initiated at midday. Triplicate samples for Net Primary Production (NPP) were spiked with 5 µCi $H^{14}CO_3^-$ and incubated for 24h. In addition to the six NPP and GPP bottles, two bottles were used as controls and spiked with 5 µCi $H^{14}CO_3^-$: one bottle was filtered immediately after addition (blank), while the other was incubated in the dark for 24h in the seawater tank (negative control).To quantify total ^{14}C activity for specific activity calculations, a subsample (125 µl) was collected from each bottle after the incubation

period. Subsequently, samples were filtered onto a 0.7µm glass fiber filter, which was placed into 20mL scintillation vials and acidified with 6N HCl for at least 24h. Radioactivity in the samples was measured by scintillation counting on a Beckman-Coulter Liquid Scintillation counter (LSC 6500), using a standard quench curve correction to derive disintegrations per minute. The errors were calculated as standard deviation of the triplicate. An estimation of the correction for respiration of unlabeled carbon during the 24h experiment was also calculated (see Notes S1).

***In situ* measurement of $\Delta O_2/Ar$ and triple oxygen isotopes**.
Samples were collected with a Go-flo bottle and transferred immediately into a 500mL custom-made pre-evacuated and pre-poisoned bottles with Louwers-Hapert (LH) valves (Emerson *et al.*, 1995). Great care was taken during the sample collection process to avoid entrainment of atmospheric oxygen. The samples were stored at ambient temperature and analyzed at Woods Hole Oceanographic Institution within 6 months. Analysis followed the method of Barkan and Luz (2003) with the modification that the GC column was 5.3 m and held at -3 °C, and that each sample was collected on a cryogenic trap at <10°K which was then warmed to room temperature and directly released into an isotope ratio mass spectrometer. The ratio O_2/Ar reflects the mass balance between NCP and gas exchange (Craig & Hayward, 1987; Emerson *et al.*, 1991), while the triple oxygen isotope measurement reflects the mass balance between GPP and gas exchange (using the equation described in Prokopenko *et al.* (2011)). The details of this approach have been described previously (Luz & Barkan, 2000; Reuer *et al.*, 2007) and are explained in Supplementary notes S2. Values for NCP and GPP were converted from µmol O_2 m^{-2} d^{-1} to µmol O_2 L^{-1} d^{-1} using the computed mixed layer depth (derived from a density difference criterion of 0.125 kg m^{-3}) or our sampling depth of 10m, whichever was greater.

Bacterial productivity and respiration.

30mL bottles were filled with seawater sub-samples. Triplicate control bottles were immediately spiked with 200µL formalin (37% formaldehyde) to stop biological activity. All bottles were then spiked with 50µL ^{3}H-thymidine. The biologically active bottles (in triplicate) were then incubated in the outdoor seawater tank for 2h. At the end of the incubation, biological activity was stopped by adding 200 µL formalin. A subsample was taken from all bottles for specific activity determination, while the remaining volume was filtered on a 0.2µM cellulose nitrate filter. The filters were dried overnight, dissolved in ethyl acetate, and counted on a Beckman-Coulter Liquid Scintillation counter (LSC 6500), with quench correction. Following (Kirchman *et al.*, 1982), the uptake rate of labelled compound v(t) is assumed proportional to the bacterial growth rate: $v(t)= \frac{1}{C} * \frac{dN(t)}{dt}$, where N is the number of cells and the conversion factor $C= 1.2 \times 10^{6}$ cells pmol^{-1} (Delille & Cahet, 1997). Bacterial production and respiration were calculated using an average value of 10 fgC cell^{-1} and a growth efficiency factor of 0.15 (Ducklow *et al.*, 2012). Errors were calculated as standard deviation of the triplicates.

Laboratory culture experiments.

Fragilariopsis cylindrus (CCMP 1102) was grown in semi continuous batch culture using 0.2 µm filtered coastal seawater supplemented with Aquil nutrients (Sunda *et al.*, 2005) under continuous light (c. 150 µE m^{-2} s^{-1}) at 0.5°C. Cells densities were counted with a Coulter Counter Z2 (Beckman Coulter Inc, Fullerton, CA). Cells were harvested during exponential phase after ~2 weeks of growth. Incubations with $H_2{}^{18}O$ in the light were performed (as described above) to yield estimates of net and gross photosynthesis as well as respiration in the light. Additional incubations were performed in the dark to derive estimates of respiration in the dark from the change in O_2 concentration.

Cyclic electron flow.

For the determination of relative cyclic electron transport rates, *Fragilariopsis cylindrus* cells in exponential growth were filtered gently and resuspended into Aquil medium with 20% w/w Ficoll. Following continuous illumination during which the redox state of P_{700} in PSI reaches steady state, the reduction rate of P_{700} was measured in the dark by fast spectrophotometry as the increase in absorbance at 700nm (JTS-10 spectrophotometer, BioLogic, France). The total number of PSI as well as the rate of their dark reduction, due to either cyclic or linear electron flow, was obtained by the technique reviewed in Alric (2010). To discriminate between the cyclic and linear electron flow, the measurements were done under two different conditions: without any inhibitor and in the presence of DCMU (3-(3,4-dichlorophenyl)-1,1-dimethylurea, 20µM) a specific inhibitor of PSII that blocks the linear flow of electrons going to PSI. To obtain the initial rate of P_{700} reduction, the spectroscopic data were fitted with an exponential function and corrected for an instrumental artefact as explained in supplemental information (Notes S3).

RESULTS

Community composition and phytoplankton biomass

The near shore waters adjacent to Palmer station are typically ice-covered in the winter. During the austral spring 2012, the ice retreated at the end of October (~ October 25th). A large bloom of phytoplankton was observed in late November-early December of 2012 (up to 45µg Chl *a* L^{-1}; Fig. 1a). Based on the analyses of three marker pigments (fucoxanthin, 19'-hexanoyloxyfucoxanthin , and alloxanthin, see Arrigo *et al*., (2000)), the phytoplankton community at the beginning of the season was equally dominated by diatoms and *Phaeocystis* (Fig. 1a). As the diatom bloom developed, the *Phaeocystis* share of the community decreased and at the peak of the bloom the population was essentially all diatoms. The bloom was interrupted by a mixing event which

306 temporarily reduced the chlorophyll concentration down to 10 µg L^{-1}
307 (on December 4th). In mid-December, the bloom crashed and
308 thereafter the phytoplankton population, then dominated by
309 cryptophytes and *Phaeocystis*, was maintained around 1-3 µg Chl *a* L^{-1}.
310 The abundance of macro-nutrients at the crash of the bloom and during
311 the rest of the season (Fig. S4) suggests that the end of the bloom and
312 thereafter control of the population was likely due to grazing (Tortell *et*
313 *al.*, 2014). In early March, a smaller bloom of diatoms and *Phaeocystis*
314 yielded chlorophyll concentration slightly above 6 µg L^{-1}.

315 **Photosynthesis and respiration during daylight**

316 To study photosynthesis and respiration in the light, incubations with
317 $H_2{}^{18}O$ were performed weekly on water collected from LTER-station B,
318 starting at midday and lasting 4 to 8h. The rates of both net and gross
319 production in the bottle are given in unit of µmol L^{-1} d^{-1} but only pertain
320 to the period of the incubation. These incubations thus included the
321 daily irradiance peak around 3PM and were all done at saturating light.
322 We observed no relationship between average PAR during the
323 incubations and the Chl *a* –normalized photosynthetic rates (Fig. S5),
324 suggesting that photoinhibition or light limitation were not occurring. .
325 Net bottle production in the light (NBP_L), defined as the difference
326 between photosynthetically produced oxygen and respiratory O_2
327 consumption by the autotrophs and heterotrophs in the bottle, was
328 measured by ΔO_2, the difference between the final and the initial O_2
329 concentration in the incubation bottle. Early in the season (before Nov
330 14^{th}), the incubations showed a net heterotrophy during daylight as
331 shown by a slightly negative NBP_L (Fig. 1b). This net heterotrophy was
332 confirmed by in situ measurement of dO_2/Ar with a Membrane Inlet
333 Mass Spectrometer (Tortell *et al.*, 2014). During the bloom (defined
334 here as the period between November 19^{th} and December 10^{th} 2012
335 when the chlorophyll was above 5 µg Chl *a* L^{-1}), we measured a very
336 high NBP_L with a maximum > 90 µmol O_2 L^{-1} d^{-1} corresponding to > 65

337 µmol C L^{-1} d^{-1} (using an average photosynthetic quotient PQ=1.39; Fig.
338 1b). For the rest of the season, NBP_L values less than 6 µmol C L^{-1} d^{-1}
339 were obtained until the second bloom, when values increase to ~18
340 µmol C L^{-1} d^{-1}.

341 In the same bottles, Gross Photosynthesis (GP; defined as the amount of
342 oxygen produced from the splitting of water during photosynthesis) was
343 also measured, independently of NBP_L, as the increased concentration
344 of $^{18}O^{16}O$ in incubations with $H_2{}^{18}O$ (see method). During most of the
345 season the measured ^{18}O-derived GP closely tracked the measured ΔO_2-
346 derived NBP_L (Fig. 2a). The correlation between the two (0.89 ± 0.08;
347 R^2=0.89) in these incubations is dominated by the high values during the
348 bloom and indicates that during several hours at midday net production
349 in the bottle was roughly 90% of GP. Thus respiration at midday during
350 the bloom, calculated as the difference of GP minus NBP_L during the
351 incubation, was only ~10% of GP. This respiration includes respiration by
352 autotrophs (mitochondrial respiration and photorespiration),
353 respiration by heterotrophs (mainly bacteria, as larger heterotrophs are
354 excluded from the incubation bottles) and potentially the reduction of
355 O_2 in the Mehler reaction. Bacterial respiration, derived from thymidine
356 incorporation measured in separate 2h incubations at midday, was less
357 than 2 µmol C L^{-1} d^{-1} during the season at 10m depth, except at the
358 crash of the bloom when it increased to ~8 µmol C L^{-1} d^{-1} (Dec 14th, see
359 Notes S4 and Fig. S6). After the crash of the first bloom, our ΔO_2
360 measurements in the incubations revealed very low overall net
361 production (see Table S1).

362 Gross photosynthesis in the ^{18}O bottle incubations varied linearly with
363 chlorophyll (Fig. 3) up to ~25 µg L^{-1}. The slope of 3.0 µmol C µg Chl a^{-1} d^{-1}
364 is similar to the values from the Antarctic reported by Westwood *et al.*
365 (2010) (4.1 ± 1.7 µmol C µg Chl a^{-1} d^{-1} between 0-25m) and by DiTullio *et*
366 *al.* (2003) (5.6 ± 4.6 µmol C µg Chl a^{-1} d^{-1} in the Antarctic zone). The
367 linearity of Figure 3, despite the variability of the light intensity among

experiments (PAR ~200 to ~670 µE m^{-2} s^{-1}), indicates that photosynthesis was likely light saturated during those incubations (see figure S5).

Photosynthesis and respiration during a light-dark cycle using ^{14}C

In order to measure net and gross primary production during a full diel cycle, 2 and 24h $^{14}CO_2$ uptake incubations were performed twice weekly starting around midday. Net Primary Production (NPP) measured in 24h experiments represents the gross carbon fixation minus DOC excretion and respiration by the autotrophs and heterotrophs present in the incubation bottles (excluding large zooplankton). A somewhat lower value for a net primary production NPP*, is obtained by subtracting from the measured NPP an estimate of the unlabeled carbon respired during the 24h incubation (see supplemental Note S1). Due to a mixing event (that was not captured by an ^{18}O incubation) those incubations showed two peaks of high net production during the bloom (Fig. 1c), reaching up to 78 µmol C L^{-1} d^{-1} on December 10th. Differences in the relative values of net production measured by ^{14}C and ^{18}O incubations result, in part, from differences in the duration of light saturation during the two types of experiments. During the rest of the season the ^{14}C based NPP values were generally less than 2 µmol C L^{-1} d^{-1}.

The average ratio of ^{14}C-NPP/^{18}O- NBP ~0.79 during the bloom and 0.20 after the crash of the bloom, illustrates the fact that the two methods measure different processes (see below). The average ratio ^{18}O-GP/^{14}C NPP ~3.57 measured for the entire season up to the second bloom is similar to previously reported values in the laboratory (Halsey *et al.*, 2013) and is within the range of the values reported from the field (Bender *et al.*, 1999; Laws *et al.*, 2000; Marra, 2007; Hamme *et al.*, 2012).

Gross primary production (GPP), which represents the CO_2 fixed by the autotrophs into new biomass, was measured in separate bottles spiked with $^{14}CO_2$ and incubated at the same time and in the same tank as NPP but for only 2h at midday. The rates are given in µmol L^{-1} d^{-1} but only pertain to the 2h period of incubation. Surprisingly, some of the measurements at the beginning of the season and during the bloom gave GPP values that were lower than the NPP. Such ratios of ^{14}C-NPP/^{14}C-GPP > 1 have been observed previously (Robinson *et al.*, 2009) and may reflect a reduced photosynthetic activity at midday.

Omitting the data where ^{14}C GPP was lower than NPP, we observe a strong correlation between NPP and GPP (Fig. 2b) with a slope of 0.61±0.05 before/during the bloom and a slope of 0.54±0.07 afterward. Those slopes are somewhat lower when respiration of unlabeled carbon is taken into account (NPP* vs GPP: 0.54 before/during the bloom and 0.24 after the bloom). Those ratios of net production to gross photosynthesis are much lower than our value of ~0.9 from the ^{18}O incubations obtained at midday. Part of the explanation is the difference in timing between the ^{18}O and ^{14}C incubations, with only the latter measurements including the dark portion of the day. Differences in the diel patterns of photosynthesis and respiration rates (Moline & Prezelin, 1996) would also lead to discrepancies between the two methods, as would excretion of some of the organic carbon (which is accounted for in the ^{18}O but not in the ^{14}C experiments).

Photosynthesis and respiration: time- integrated *in situ* measurements

The triple oxygen isotope method provides an *in situ* measure of time-integrated gross and net production of the whole community, without any exclusion or constraints linked to bottle incubations (Luz & Barkan, 2000). Net community production in this case is derived from the supersaturation of O_2 compared to Ar which represents the balance of photosynthesis, respiration and gas exchange (computed using a wind-speed dependent parameterization of mixed layer gas exchange

coefficients according to Wanninkhof (1992)). Gross photosynthesis in the mixed layer is calculated from the isotopic composition of the O_2 pool, which is determined by the gross O_2 fluxes associated with photosynthesis (splitting of water) and air-sea exchange. The calculations of NCP and GPP were made considering that the samples were within the mixed layer and that oxygen was at steady state, except during the peak of the bloom when the changing isotopic ratios were taken into account in order to calculate rates without necessitating the steady state assumption (Kaiser, 2011; Prokopenko *et al.*, 2011). In addition, the calculations of NCP and GPP during the bloom were made considering that the sampling depth of 10m was either below the mixed layer (as indicated by the density profiles; Fig. S2) or possibly within it (as indicated by the Ekman depth; Brody and Lozier (2014)). Details of the calculations to obtain NCP, GPP and their ratios, using different hypothesis of steady state and mixed layer conditions, can be found in Tables S2 and S3 and supplemental notes S2. No matter what the method (i.e. steady-state or time-varying, within mixed layer or below it), the rates of GPP and NCP during the bloom period are much higher than the rates of GPP and NCP during the rest of the season.

Qualitatively, the triple oxygen isotope-derived NCP and GPP estimates (Fig. 1d) resemble those from ^{14}C incubations exhibiting two peaks during the bloom and remaining low afterward (except for an unexplained peak in GPP on January 8th). The absolute values in Fig. 1d however are lower than in Fig. 1b,c. This is in part due to the inherent time and space averaging of the triple oxygen isotope method, which necessarily smoothes out the high values. This integrated measure of NCP demonstrates that the system never reached a sustained period of net heterotrophy before or after the bloom with only a few values of NCP slightly below zero.

The NCP/GPP ratio measured with the dO_2/Ar and triple oxygen isotope technique started with values ~0.25 at the beginning of spring and

459 increased to values above 0.6 during the two peaks of the bloom
460 (regardless of the assumption made regarding the depth of the mixed
461 layer). These high ratios observed in both NCP/GPP from *in situ*
462 measurements and NPP/GPP from ^{14}C data, indicated that community
463 respiration was largely controlled by the microorganisms that were
464 sampled in the bottles, as opposed to large grazers that would have
465 been excluded. Thymidine incorporation measurements indicate very
466 low bacterial production and respiration before and during the bloom
467 (Fig. S6), implying that much of the respiration was attributable to the
468 phytoplankton. Just at the crash of the bloom the O_2 NCP/GPP
469 decreased to low and possibly negative values as expected and
470 confirmed by estimates of high bacterial respiration based on thymidine
471 incorporation data (Fig. S6). During the rest of the season we observed a
472 low positive NCP/GPP ratio ranging between ~-0.1 and ~0.1, much lower
473 than the ratio of 0.54 obtained from the ^{14}C data. This large difference
474 likely reflects the activity of large grazers which are excluded from the
475 ^{14}C incubation bottles but keep the algal population and the net
476 community production low (Tortell *et al.*, 2014). Our observations thus
477 suggest that autotrophic respiration dominated community O_2
478 consumption during the pre-bloom and bloom phases of the seasonal
479 cycle, while large grazers (*e.g.,* Krill) accounted for most of the
480 community respiration during the later months.

481 **Physiological data from the polar diatom *Fragilariopsis cylindrus***

482 Since diatoms were the major taxa during the bloom, we conducted
483 experiments with the psychrophilic organism *Fragilariopsis cylindrus* in
484 laboratory cultures maintained at 0.5°C under continuous light. $H_2{}^{18}O$
485 incubations (~9h) on those light adapted cells gave values of 0.38 and
486 0.12 pmol O_2 $cell^{-1}$ d^{-1} for gross photosynthesis and respiration in the
487 light respectively, while incubations in the dark gave a value of 0.07
488 pmol O_2 $cell^{-1}$ d^{-1} for respiration in the dark (Fig. 4a). Based on these
489 data, we calculated a ratio for the daily integrated net and gross

production for a diel cycle with 20h/4h L/D (similar to the diel cycle during the bloom) of NP_D /GP of 0.65. This value represents an average value for the light period since our cultures were grown under continuous light and thus not synchronized to a diel cycle like the community in the WAP. Nonetheless, this value is very close to the values we obtained in the field during the bloom from *in situ* measurements (Fig. 2c). To the extent that the ratio obtained with *F.cylindrus* can be extrapolated to the diatoms in the WAP, these results provide further evidence that the community respiration measured during the bloom was dominated by the phytoplankton. This is consistent with our estimations of low heterotrophic respiration in the field based on thymidine incorporation rates (see above) and with previous studies (Ducklow *et al.*, 2012).

It has been suggested that cyclic electron flow (CEF) generates substantial ATP in psychrophilic green algae from Antarctic lakes (Morgan-Kiss *et al.*, 2002; Dolhi *et al.*, 2013). Such a mechanism could help explain the very low respiration rates we observed at midday in the field (with the $H_2{}^{18}O$ incubations) as well as the previously reported high concentration of ATP in psychrophilic organisms (Napolitano & Shain, 2005). In CEF, light absorption and charge separation in PSI is followed by an electron transfer back to the b6f complex, via a ferredoxin, and the beginning of a cycle through the plastoquinone pool (Falkowski & Raven, 2007). Each cycle transports protons from the stroma to the lumen, generating a proton gradient, which leads to the production of ATP via the ATP synthase in the thylakoid membrane (see Eberhard *et al.* (2008) for review). Re-reduction of PSI can occur through the linear flow of electron from PSII or from CEF. Using laboratory cultures of *F. cylindrus*, we obtained the first estimates of the relative importance of CEF and linear electron flow in a psychrophilic diatom. The reduction rates of the PSI pool in the presence and absence of DCMU (an inhibitor of linear electron flow) were compared using a fast spectrophotometric

method (see Alric (2010) for review). The maintenance of a rapid reduction rate of PSI (~ 30 $e^- s^{-1}$) in *F. cylindrus* (at 0°C) in the presence of DCMU (Fig. 4b) is indicative of an active CEF. In contrast, for *T. weissflogii* at 25°C the electron flow decreased to low values in the presence of DCMU (< 15 $e^- s^{-1}$; Fig. 4b) indicating minimal CEF in this species under these conditions. Such low rate of PSI reduction in the presence of DCMU in *T. weissflogii* could also result from the breakdown of starch to produce NADPH (Alric *et al.* (2010)).

DISCUSSION

We used three different techniques to measure primary production during our field season: two in vitro techniques (^{18}O incubations, ^{14}C incubations) and one *in situ* method (dO_2/Ar and triple oxygen isotopes). These techniques measure different parameters over different time periods and provide complementary insights into the processes responsible for the metabolic balance of the planktonic ecosystem. Notably, all three methods demonstrated a high level of net production during the diatom spring bloom, which, although not atypical, appears to have been one of the largest on record during the 25 years of observation at the Palmer Station LTER site (http://oceaninformatics.ucsd.edu/datazoo/data/pallter/datasets). According to the LTER data archive, there were 15 years between 1991 and 2011 when the chlorophyll concentrations exceeded 10 µg L^{-1}, and 8 when they exceeded 30 µg L^{-1}. During our field season, the chlorophyll concentration reached 45 µg.L^{-1}, concomitant with a gross production rate of 75 µmol C L^{-1} d^{-1} (Fig. 1b). Using the relationship derived between ^{18}O-GP and chlorophyll (Fig. 3), we estimate that the bloom accounted for nearly 60% of the gross production during the entire summer season. This particular bloom provided an opportunity to better understand the processes that allow high primary productivity in very cold waters. Our data indicate that heterotrophic processes played a minimal role during the spring bloom and that all metabolic processes

552 were dominated by autotrophs. This explains why both ^{14}C and the *in*
553 *situ* (dO_2/Ar and $^{17}\Delta$) measurements, gave similarly high ratios of
554 net/gross production, with maximum values of greater than 0.54. For
555 comparison, most published ratios of net to gross production based on
556 dO_2/Ar and $^{17}\Delta$ data in low temperature seawater are below 0.2 (Castro-
557 Morales *et al.*, 2013), (Juranek *et al.*, 2012), with a few values above:
558 0.35 on average during spring bloom conditions in the subpolar North
559 Atlantic Ocean (Quay *et al.*, 2012), up to 0.43 in the WAP (Huang *et al.*,
560 2012) and ~0.50 in the Bering Sea (Prokopenko et al. 2011).

561 Taken at face value, the results of our ^{18}O incubations during the
562 bloom indicate that most of the electrons obtained from the splitting of
563 water result in net carbon fixation during midday. This means that
564 photorespiration and mitochondrial respiration, as well as the Mehler
565 reaction, were kept to a minimum in the diatoms at Palmer station at
566 midday. The extent of photorespiration depends on the relative affinity
567 of Rubisco for CO_2 and O_2 which are competing for binding at the active
568 site. As in higher plants, the O_2 turnover rate in the Rubisco of diatoms
569 is slower than that of CO_2. The Rubisco of diatoms can also exhibit a
570 half-saturation constant for oxygen up to 8 times that of higher plants
571 (Badger *et al.*, 1998). Further, it has been shown in plants (Tcherkez *et*
572 *al.*, 2006), and in phytoplankton (Haslam *et al.*, 2005) that low
573 temperature increases the specificity of Rubisco for CO_2 over O_2.
574 Together with an efficient CCM in the cells (see Kranz *et al.* (accepted)),
575 the increased CO_2 specificity of Rubisco (Young *et al.*, accepted) should
576 act to maintain low photorespiration relative to C fixation in
577 psychrophilic diatoms.

578 Cyclic electron flow, CEF, allows cells to produce ATP directly from
579 sunlight without evolving oxygen or fixing carbon, and independently of
580 mitochondrial respiration. To the extent that this mechanism for ATP
581 production depends principally on photochemical processes, it should
582 be less sensitive to temperature than the multiple enzymatic reactions

583 of the Krebs cycle. This requires that the activity of the enzymes
584 involved in the CEF and ensuing ATP production be maintained high
585 either by adaptation to cold or by a higher protein concentration. In
586 particular the activity of the ATP synthase in the thylakoid membrane
587 must be high enough. A significant role for cyclic electron flow has been
588 reported previously in an Antarctic green alga from Lake Bonney (Dolhi
589 *et al.*, 2013). The Mehler reaction is in competition with the cyclic
590 electron flow in PSI. Our ^{18}O incubation data during the bloom imply
591 that like photorespiration, mitochondrial respiration and the Mehler
592 reaction are minimal at midday in Antarctic diatom; this may be
593 associated with an intense CEF activity. Our laboratory experiment with
594 *F. cylindrus* confirmed that this process is indeed physiologically
595 important in this polar diatom. High intracellular ATP concentrations
596 previously reported in two psychrophilic green algae (Napolitano &
597 Shain, 2005) would also be consistent with a high CEF activity.
598 Interestingly, in those psychrophilic species, ATP concentrations were
599 reported to increase with decreasing temperature whereas the opposite
600 trend is observed in mesophilic and thermophilic organisms.

601 The very low respiration measured during our ^{18}O incubation during
602 the bloom at midday (~10% of GP) is somewhat difficult to reconcile
603 with the ^{14}C incubation and *in situ* measurements that show net/gross
604 ratio on the order of 0.6 (Fig. 2). If such a low respiration were
605 maintained for the whole daylight period, it would mean that 30% of
606 the photosynthate would have to be respired during the night to
607 reconcile the numbers. This seems difficult considering that the night at
608 Palmer lasted only 4h during the height of the phytoplankton bloom.
609 Alternatively, respiration by autotrophs (or heterotrophs) may also have
610 been higher during early and late daylight hours than during midday.
611 This would be consistent with a scenario in which the cells exploit the
612 high photon flux at midday to generate ATP through cyclic electron
613 flow. Conceivably, an intense CEF activity at the expense of linear
614 electron flow during periods of high light could also explain low GPP

615 measured in short term ^{14}C experiments. Clearly, additional information
616 on the diel cycle of photosynthesis and CEF activity of psychrophilic
617 diatoms should help us understand how the ratio of net/gross
618 photosynthesis varies in the course of a day.

619 From an ecological perspective, an important implication of our
620 data is the low ratio of community respiration/ gross primary
621 production during the diatom spring bloom at Palmer station. Based on
622 our laboratory data with *F.cylindrus* we hypothesize that part of the
623 reason why phytoplankton may be able to maintain relatively high
624 productivity at low temperature even when their respiration rate falls
625 (as it does at midday) is because they can generate ATP through cyclic
626 electron flow. More generally the overall trend of decreasing R/P with
627 decreasing temperature (Regaudie-de-Gioux & Duarte, 2012), that is a
628 characteristic of ecosystems dominated by autotrophs results not just
629 from the temperature-dependence of the rates of photochemical and
630 biochemical reactions but must also reflect particular adaptive
631 strategies, such as CEF and the change in the concentration and
632 substrate affinity of key enzymes such as Rubisco (Young *et al.*,
633 accepted). A better understanding of these strategies would allow us to
634 foresee the likely changes in the net productivity of marine ecosystems
635 at high latitudes which are being subjected to rapid climate change.

636 **Acknowledgments**

637 We would like to acknowledge the exceptional assistance and support
638 of the United States Antarctic Program support staff at Palmer station
639 as well as the entire Palmer LTER science team. We are particularly
640 thankful to Prof. Hugh Ducklow for his help with bacteria productivity
641 measurements. We also thank Prof. John Dacey for his assistance during
642 sampling, Stefanie Strebel for her assistance at Palmer station, and Zoe
643 Sandwith for her assistance in measuring triple oxygen isotopes. We
644 are very grateful to Prof. Paul Falkowski letting us use his facilities and
645 instrument to measure cyclic electron flow, and to Dr. Benjamin Bailleul

646 for his expert advice and patient help for cyclic electron flow
647 measurements. This study was supported by funds from the US National
648 Science Foundation (Award numbers 1040965 and 1043593). Funding to
649 PDT was provided by the Natural Science and Engineering Research
650 Council of Canada.

References

Alric J. 2010. Cyclic electron flow around photosystem I in unicellular green algae. *Photosynthesis research* **106**(1-2): 47-56.

Alric J, Lavergne J, Rappaport F. 2010. Redox and ATP control of photosynthetic cyclic electron flow in< i> Chlamydomonas reinhardtii</i>(I) aerobic conditions. *Biochimica et Biophysica Acta (BBA)-Bioenergetics* **1797**(1): 44-51.

Arrigo KR, DiTullio GR, Dunbar RB, Robinson DH, VanWoert M, Worthen DL, Lizotte MP. 2000. Phytoplankton taxonomic variability in nutrient utilization and primary production in the Ross Sea. *Journal of Geophysical Research: Oceans (1978–2012)* **105**(C4): 8827-8846.

Arrigo KR, van Dijken G, Long M. 2008a. Coastal Southern Ocean: A strong anthropogenic CO_2 sink. *Geophysical Research Letters* **35**(21): L21602.

Arrigo KR, van Dijken GL, Bushinsky S. 2008b. Primary production in the Southern Ocean, 1997–2006. *Journal of Geophysical Research: Oceans (1978–2012)* **113**(C8).

Badger MR, Andrews TJ, Whitney S, Ludwig M, Yellowlees DC, Leggat W, Price GD. 1998. The diversity and coevolution of Rubisco, plastids, pyrenoids, and chloroplast-based CO_2-concentrating mechanisms in algae. *Canadian Journal of Botany* **76**(6): 1052-1071.

Barkan E, Luz B. 2003. High-precision measurements of 17O/16O and 18O/16O of O2 and O2/Ar ratio in air. *Rapid communications in mass spectrometry* **17**(24): 2809-2814.

Bender M, Orchardo J, Dickson M-L, Barber R, Lindley S. 1999. In vitro O_2 fluxes compared with ^{14}C production and other rate terms during the JGOFS Equatorial Pacific experiment. *Deep Sea Research Part I: Oceanographic Research Papers* **46**(4): 637-654.

Brody SR, Lozier MS. 2014. Changes in dominant mixing length scales as a driver of subpolar phytoplankton bloom initiation in the North Atlantic. *Geophysical Research Letters* **41**(9): 3197–3203.

Castro-Morales K, Cassar N, Shoosmith DR, Kaiser J. 2013. Biological production in the Bellingshausen Sea from oxygen-to-argon ratios and oxygen triple isotopes. *Biogeosciences* **10**(4): 2273-2291.

Craig H, Hayward T. 1987. Oxygen supersaturation in the ocean: Biological versus physical contributions. *Science* **235**(4785): 199-202.

Culberson CH, Huang S. 1987. Automated amperometric oxygen titration. *Deep Sea Research Part A. Oceanographic Research Papers* **34**(5): 875-880.

Delille D, Cahet G. 1997. Determination of conversion factors for estimation of subantarctic marine bacterial production measured by H-thymidine Incorporation methodology. *Aquatic microbial ecology* **13**(1): 121-125.

DiTullio GR, Geesey ME, Jones DR, Daly KL, Campbell L, Smith WO. 2003. Phytoplankton assemblage structure and primary productivity along 170 degrees W in the South Pacific Ocean. *Marine Ecology Progress Series* **255**: 55-80.

Dolhi JM, Maxwell DP, Morgan-Kiss RM. 2013. Review: the Antarctic Chlamydomonas raudensis: an emerging model for cold adaptation of photosynthesis. *Extremophiles* **17**(5): 711-722.

Ducklow HW, Baker K, Martinson DG, Quetin LB, Ross RM, Smith RC, Stammerjohn SE, Vernet M, Fraser W. 2007. Marine pelagic ecosystems: the west Antarctic Peninsula. *Philosophical Transactions of the Royal Society B: Biological Sciences* **362**(1477): 67-94.

Ducklow HW, Schofield O, Vernet M, Stammerjohn S, Erickson M. 2012. Multiscale control of bacterial production by phytoplankton dynamics and sea ice along the western Antarctic Peninsula: a regional and decadal investigation. *Journal of Marine Systems* **98**: 26-39.

Eberhard S, Finazzi G, Wollman F-A. 2008. The dynamics of photosynthesis. *Annual review of genetics* **42**: 463-515.

Emerson S, Quay P, Stump C, Wilbur D, Knox M. 1991. O2, Ar, N2, and 222Rn in surface waters of the subarctic ocean: Net biological O2 production. *Global Biogeochemical Cycles* **5**(1): 49-69.

Emerson S, Quay P, Stump C, Wilbur D, Schudlich R. 1995. Chemical tracers of productivity and respiration in the subtropical Pacific Ocean. *Journal of Geophysical Research: Oceans (1978–2012)* **100**(C8): 15873-15887.

Everitt D, Wright S, Volkman J, Thomas D, Lindstrom E. 1990. Phytoplankton community compositions in the western equatorial Pacific determined from chlorophyll and carotenoid pigment distributions. *Deep Sea Research Part A. Oceanographic Research Papers* **37**(6): 975-997.

Falkowski PG, Raven JA. 2007. *Aquatic photosynthesis*: Princeton University Press.

Halsey KH, O'Malley RT, Graff JR, Milligan AJ, Behrenfeld MJ. 2013. A common partitioning strategy for photosynthetic products in evolutionarily distinct phytoplankton species. *New Phytologist* **198**(4): 1030-1038.

Hamme RC, Cassar N, Lance VP, Vaillancourt RD, Bender ML, Strutton PG, Moore TS, DeGrandpre MD, Sabine CL, Ho DT. 2012. Dissolved O_2/Ar and other methods reveal rapid changes in productivity during a Lagrangian experiment in the Southern Ocean. *Journal of Geophysical Research: Oceans (1978–2012)* **117**: C00F12.

Haslam RP, Keys AJ, Andralojc PJ, Madgwick PJ, Inger A, Grimsrud A, Eilertsen HC, Parry MA 2005. Specificity of diatom Rubisco. In: Omasa K, Nouchi I, De Kok LJ eds. *Plant responses to air pollution and global change*. Tokyo, Japan: Springer, 157-164.

Huang K, Ducklow H, Vernet M, Cassar N, Bender ML. 2012. Export production and its regulating factors in the West Antarctica Peninsula region of the Southern Ocean. *Global Biogeochemical Cycles* **26**(2).

Juranek L, Quay P. 2013. Using triple isotopes of dissolved oxygen to evaluate global marine productivity. *Annual review of marine science* **5**: 503-524.

Juranek L, Quay P, Feely R, Lockwood D, Karl D, Church M. 2012. Biological production in the NE Pacific and its influence on air-sea CO_2 flux: Evidence from dissolved oxygen isotopes and O_2/Ar. *Journal of Geophysical Research: Oceans (1978–2012)* **117**: C05022.

Kaiser J. 2011. Technical note: Consistent calculation of aquatic gross production from oxygen triple isotope measurements. *Biogeosciences* **8**(7): 1793-1811.

Kirchman D, Ducklow H, Mitchell R. 1982. Estimates of bacterial growth from changes in uptake rates and biomass. *Applied and Environmental Microbiology* **44**(6): 1296-1307.

Kranz SA, Young JN, Hopkinson BM, Goldman JA, Tortell PD, MM MF. accepted. Low temperature reduces the energetic requirement for the CO2 concentrating mechanism in diatoms. *New Phytologist*.

Langdon C. 1984. Dissolved oxygen monitoring system using a pulsed electrode: design, performance, and evoluation. *Deep Sea Research Part A. Oceanographic Research Papers* **31**(11): 1357-1367.

Laws EA, Falkowski PG, Smith WO, Ducklow H, McCarthy JJ. 2000. Temperature effects on export production in the open ocean. *Global Biogeochemical Cycles* **14**(4): 1231-1246.

Luz B, Barkan E. 2000. Assessment of oceanic productivity with the triple-isotope composition of dissolved oxygen. *Science* **288**(5473): 2028-2031.

Marra J 2007. Approaches to the Measurement of Plankton Production. In: Williams PJlB, Thomas DN, Reynolds CS eds. *Phytoplankton Productivity: Carbon Assimilation in Marine and Freshwater Ecosystems*. Oxford, UK: Blackwell Science Ltd, 78-108.

Meredith MP, King JC. 2005. Rapid climate change in the ocean west of the Antarctic Peninsula during the second half of the 20th century. *Geophysical Research Letters* **32**: L19604.

Mock T, Hoch N. 2005. Long-term temperature acclimation of photosynthesis in steady-state cultures of the polar diatom Fragilariopsis cylindrus. *Photosynthesis research* **85**(3): 307-317.

Moline MA, Prezelin BB. 1996. High-resolution time-series data for 1991/1992 primary production and related parameters at a Palmer LTER coastal site: implications for modeling carbon fixation in the Southern Ocean. *Polar Biology* **17**(1): 39-53.

Montes-Hugo M, Doney SC, Ducklow HW, Fraser W, Martinson D, Stammerjohn SE, Schofield O. 2009. Recent Changes in

Phytoplankton Communities Associated with Rapid Regional Climate Change Along the Western Antarctic Peninsula. *Science* **323**(5920): 1470-1473.

Morgan-Kiss RM, Ivanov AG, Huner NP. 2002. The Antarctic psychrophile, Chlamydomonas subcaudata, is deficient in state I–state II transitions. *Planta* **214**(3): 435-445.

Morgan-Kiss RM, Priscu JC, Pocock T, Gudynaite-Savitch L, Huner NP. 2006. Adaptation and acclimation of photosynthetic microorganisms to permanently cold environments. *Microbiology and Molecular Biology Reviews* **70**(1): 222-252.

Napolitano MJ, Shain DH. 2005. Quantitating adenylate nucleotides in diverse organisms. *Journal of biochemical and biophysical methods* **63**(1): 69-77.

Padilla-Gamino JL, Carpenter RC. 2007. Seasonal acclimatization of Asparagopsis taxiformis (Rhodophyta) from different biogeographic regions. *Limnology and oceanography* **52**(2): 833-842.

Parry ML. 2007. *Climate Change 2007: impacts, adaptation and vulnerability: contribution of Working Group II to the fourth assessment report of the Intergovernmental Panel on Climate Change*: Cambridge University Press.

Pinckney J, Paerl H, Harrington M, Howe K. 1998. Annual cycles of phytoplankton community-structure and bloom dynamics in the Neuse River Estuary, North Carolina. *Marine biology* **131**(2): 371-381.

Prokopenko MG, Pauluis OM, Granger J, Yeung LY. 2011. Exact evaluation of gross photosynthetic production from the oxygen triple-isotope composition of O_2: Implications for the net-to-gross primary production ratios. *Geophysical Research Letters* **38**: L14603.

Quay P, Stutsman J, Steinhoff T. 2012. Primary production and carbon export rates across the subpolar N. Atlantic Ocean basin based on triple oxygen isotope and dissolved O2 and Ar gas measurements. *Global Biogeochemical Cycles* **26**: GB2003.

Regaudie-de-Gioux A, Duarte CM. 2012. Temperature dependence of planktonic metabolism in the ocean. *Global Biogeochemical Cycles* **26**: GB1015.

Reuer MK, Barnett BA, Bender ML, Falkowski PG, Hendricks MB. 2007. New estimates of Southern Ocean biological production rates from O_2/Ar ratios and the triple isotope composition of O_2. *Deep Sea Research Part I: Oceanographic Research Papers* **54**(6): 951-974.

Robinson C, Tilstone GH, Rees AP, Smyth TJ, Fishwick JR, Tarran GA, Luz B, Barkan E, David E. 2009. Comparison of in vitro and in situ plankton production determinations. *Aquatic microbial ecology* **54**(1): 13-34.

Staehr PA, Birkeland MJ. 2006. Temperature acclimation of growth, photosynthesis and respiration in two mesophilic phytoplankton species. *Phycologia* **45**(6): 648-656.

Sunda WG, Price NM, Morel FM 2005. Trace metal ion buffers and their use in culture studies. In: Anderson RA ed. *Algal culturing techniques*. New York, USA: Elsevier Academic Press, 35-63.

Tcherkez GG, Farquhar GD, Andrews TJ. 2006. Despite slow catalysis and confused substrate specificity, all ribulose bisphosphate carboxylases may be nearly perfectly optimized. *Proceedings of the National Academy of Sciences* **103**(19): 7246-7251.

Tortell PD, Asher EC, Ducklow HW, Goldman JA, Dacey JW, Grzymski JJ, Young JN, Kranz SA, Bernard KS, Morel FM. 2014. Metabolic balance of coastal Antarctic waters revealed by autonomous pCO2 and ΔO2/Ar measurements. *Geophysical Research Letters*: doi: 10.1002/2014GL061266.

Valentini R, Matteucci G, Dolman A, Schulze E-D, Rebmann C, Moors E, Granier A, Gross P, Jensen N, Pilegaard K. 2000. Respiration as the main determinant of carbon balance in European forests. *Nature* **404**(6780): 861-865.

Wanninkhof R. 1992. Relationship between wind speed and gas exchange over the ocean. *Journal of Geophysical Research: Oceans (1978–2012)* **97**(C5): 7373-7382.

Welschmeyer NA. 1994. Fluorometric analysis of chlorophyll a in the presence of chlorophyll b and pheopigments. *Limnology and oceanography* **39**(8): 1985-1992.

Westwood KJ, Brian Griffiths F, Meiners KM, Williams GD. 2010. Primary productivity off the Antarctic coast from 30°–80° E; BROKE-West survey, 2006. *Deep Sea Research Part II: Topical Studies in Oceanography* **57**(9): 794-814.

Young JN, Goldman JA, Kranz SA, Tortell PD, Morel FM. accepted. Slow carboxylation of Rubisco constrains the maximum rate of carbon fixation during Antarctic phytoplankton blooms. *New Phytologist*.

Yvon-Durocher G, Caffrey JM, Cescatti A, Dossena M, del Giorgio P, Gasol JM, Montoya JM, Pumpanen J, Staehr PA, Trimmer M. 2012. Reconciling the temperature dependence of respiration across timescales and ecosystem types. *Nature* **487**: 472–476.

Figure legends

Figure 1: (a) Chl *a* and community composition for three taxa during the season. Diatoms are represented by the purple area, *Phaeocystis* by the orange area, cryptophytes by the green area. All areas are extrapolated from discrete measurements. Chl *a* is represented by the dark green curve. Error bars represent standard deviation of duplicates. (b) Results from day-time incubations with $H_2{}^{18}O$. **Blue circle**: net bottle production in the light (NBP_L) defined as ($[O_2]_{final}$-$[O_2]_{initial}$). **Green triangle**: Gross Photosynthesis (GP) defined as the production rate of [$^{18}O^{16}O$]. **Red downward triangle**: respiration in the light (R_L) defined as R_L=GP-NBP_L. Error bars represent standard deviation of duplicates. All rates are normalized for one day but only pertain to the period of incubation. The left and right axis are stoichiometrically equivalent with a photosynthetic quotient PQ=1.4 (c) Results from incubations with ^{14}C. **Blue circle**: net primary production (NPP), measured from 24h incubations. **Green triangle**: Gross Primary Production (GPP), measured from 2h incubations. GPP rates are normalized for one day but only pertain to the period of incubation. The values have been converted from carbon fixation to oxygen evolution using a PQ=1.4. Error bars represent standard deviation of triplicates. (d) Results from the *in situ* measurements. **Blue**: Net Community Production (NCP), derived from dO_2/Ar. **Green**: Gross Primary production (GPP), derived from triple oxygen isotope. Filled triangles and filled circle have been calculated assuming steady state conditions and that samples were within the mixed layer. For the two peaks of the bloom: open triangles and circles assume non steady-state and samples within the mixed layer. Filled downward triangles and squares assume non steady-state and samples below the mixed layer. No point is shown for Dec 5th as we could not account for the vertical mixing on that date. Error bars represent standard deviation of duplicates.

907

908 **Figure 2**: Relation between Gross Primary Production (GPP) and Net
909 Community Production (NCP) studied with three different
910 techniques. **Open circles**: values before and during the bloom. **Red**
911 **filled circles**: values after the bloom. **Black filled circles**: are
912 NCP/GPP ratios. (a) Incubations in the light only - $\Delta O_2/^{18}O$ method.
913 The values have been converted from oxygen evolution to carbon
914 fixation using a photosynthetic quotient PQ=1.4. Error bars represent
915 standard deviation of duplicates. (b) Incubations during a light-dark
916 cycle - ^{14}C method (24h and 2h incubations). The inset is a blow-up of
917 the data obtained after the bloom. Error bars represent standard
918 deviation of triplicates. (c) Ratio of NCP/GPP from *in situ*
919 measurements (dO_2/Ar and $^{17}\Delta$). **Black circles** assume steady state
920 and samples within the mixed layer. **Gray squares** assume non-
921 steady state and samples below the mixed layer. **Blue triangles**
922 assume non steady-state and samples above the mixed layer. Error
923 bars represent standard deviation of duplicates.
924
925 **Figure 3**: Correlation of ^{18}O derived-Gross photosynthesis (converted
926 in carbon unit using PQ values obtained for each samples as
927 explained in material and methods) and Chl *a*. Error bars represent
928 standard deviation of duplicates.
929
930 **Figure 4**: (a) Gross photosynthesis and respirations of *Fragilariopsis*
931 *cylindrus*. Incubation with $H_2{}^{18}O$ gives gross photosynthesis and
932 respiration in the light (mitochondrial respiration in the light +
933 photorespiration). Incubation in the dark gives mitochondrial
934 respiration in the dark. From those results we calculated a net
935 photosynthesis over a light:dark diel cycle of 20:4. Error bars
936 represent standard deviation of duplicates. (b) Relative electron flow

through PSI in the presence (white bars) and absence (black bars) of DCMU – comparison of *F. cylindrus* and *Thalassiosira weissflogii*. The maintenance of a high electron flow in the presence of DCMU in *F. cylindrus* is indicative of an active cyclic electron flow. Error bars represent standard deviation of duplicates.

Supplemental figures

Supplemental figure 1: map of the sampling region around Palmer station

Supplemental figure 2: Depth profiles of temperature, salinity and density at LTER-station B.

Supplemental figure 3: Mixed layer depths throughout the season determined by density profiles.

Supplemental figure 4: Concentrations of major nutrients throughout the season (CO_2 in µmol kg SW^{-1} and NO_3^-, SiO_2, PO_4^{3-} in µmol L^{-1}).

Supplemental figure 5: Chlorophyll a normalized gross photosynthesis (as measured with ^{18}O incubations) versus the average PAR during the incubation.

Supplemental figure 6: Bacterial respiration during the season (10m depth, LTER - station B) measured with thymidine incorporation

Supplemental table 1: Summary of data from incubations with $H_2{}^{18}O$.

Supplemental table 2: Summary of data to estimate Gross and Net production from dO_2/Ar and triple isotope composition

Supplemental table 3: Non steady states rates of Gross and Net community production assuming the samples are below or above the mixed layer.

Note S1: ^{14}C net primary production – correction for the respiration (R) of the unlabelled carbon during the 24h incubations

Note S2: Determining GPP and NCP Rates from triple oxygen isotope and dO_2/Ar

Note S3: Electron flow measurements – correction of the artefact

Note S4 Bacteria productivity – thymidine measurements

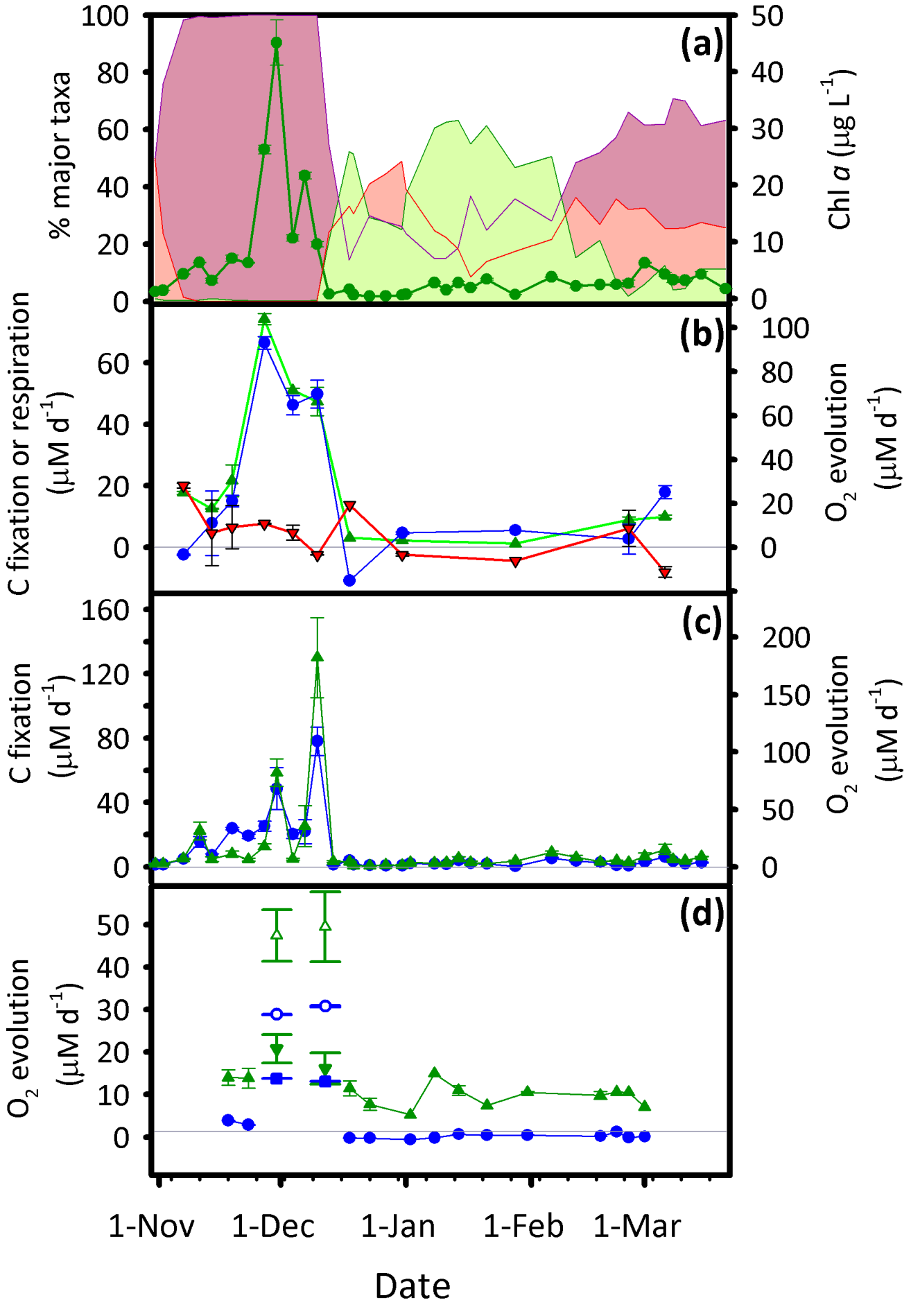
(a)
% major taxa
Chl a (µg L-1)
(b)
C fixation or respiration (µM d-1)
O2 evolution (µM d-1)
(c)
C fixation (µM d-1)
O2 evolution (µM d-1)
(d)
O2 evolution (µM d-1)
1-Nov
1-Dec
1-Jan
1-Feb
1-Mar
Date

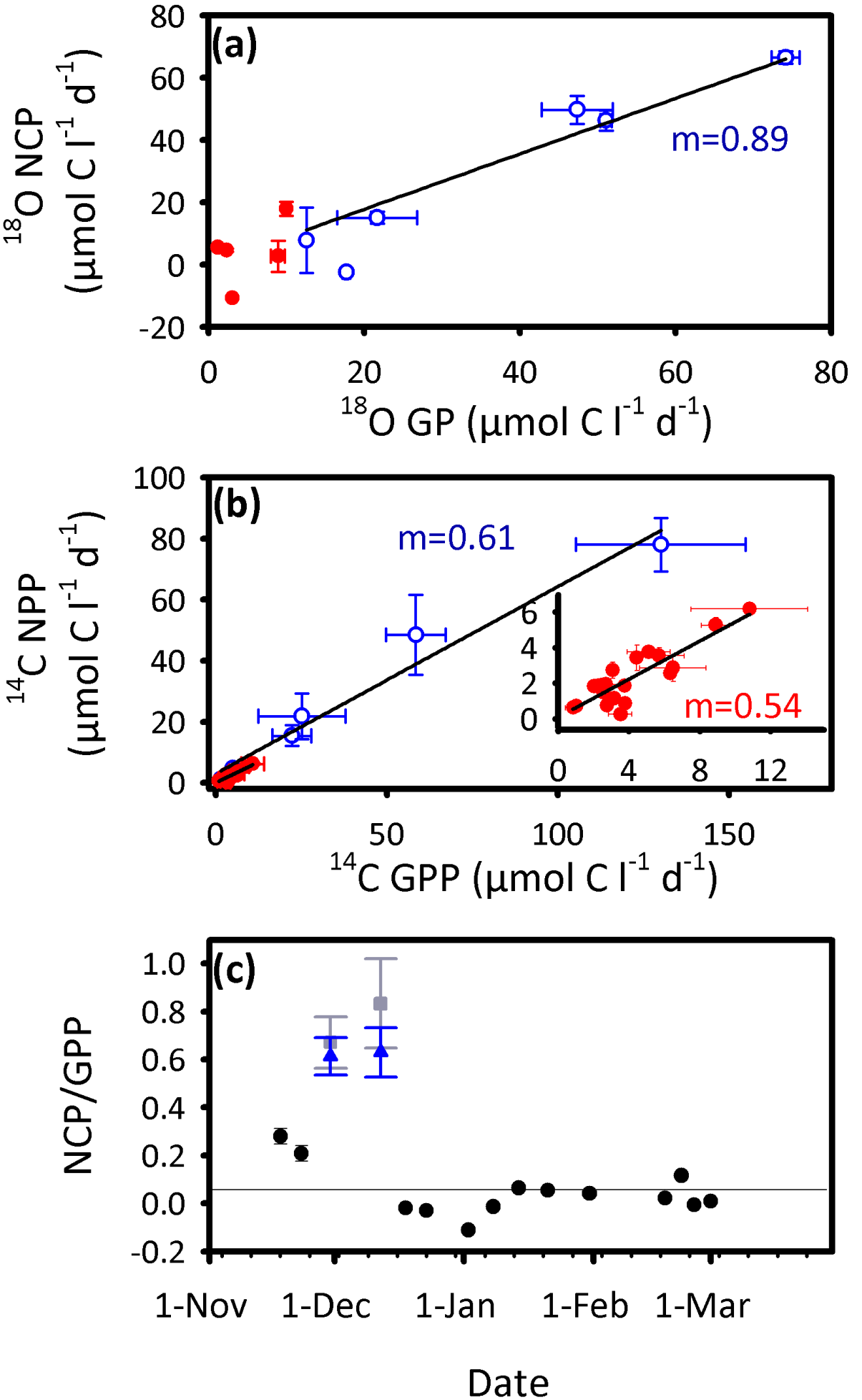
(a)
m=0.89
^{18}O NCP (µmol C l^{-1} d^{-1})
^{18}O GP (µmol C l^{-1} d^{-1})
80
60
40
20
0
-20
0
20
40
60
80
(b)
m=0.61
m=0.54
^{14}C NPP (µmol C l^{-1} d^{-1})
^{14}C GPP (µmol C l^{-1} d^{-1})
100
80
60
40
20
0
0
50
100
150
6
4
2
0
0
4
8
12
(c)
NCP/GPP
1.0
0.8
0.6
0.4
0.2
0.0
-0.2
1-Nov
1-Dec
1-Jan
1-Feb
1-Mar
Date

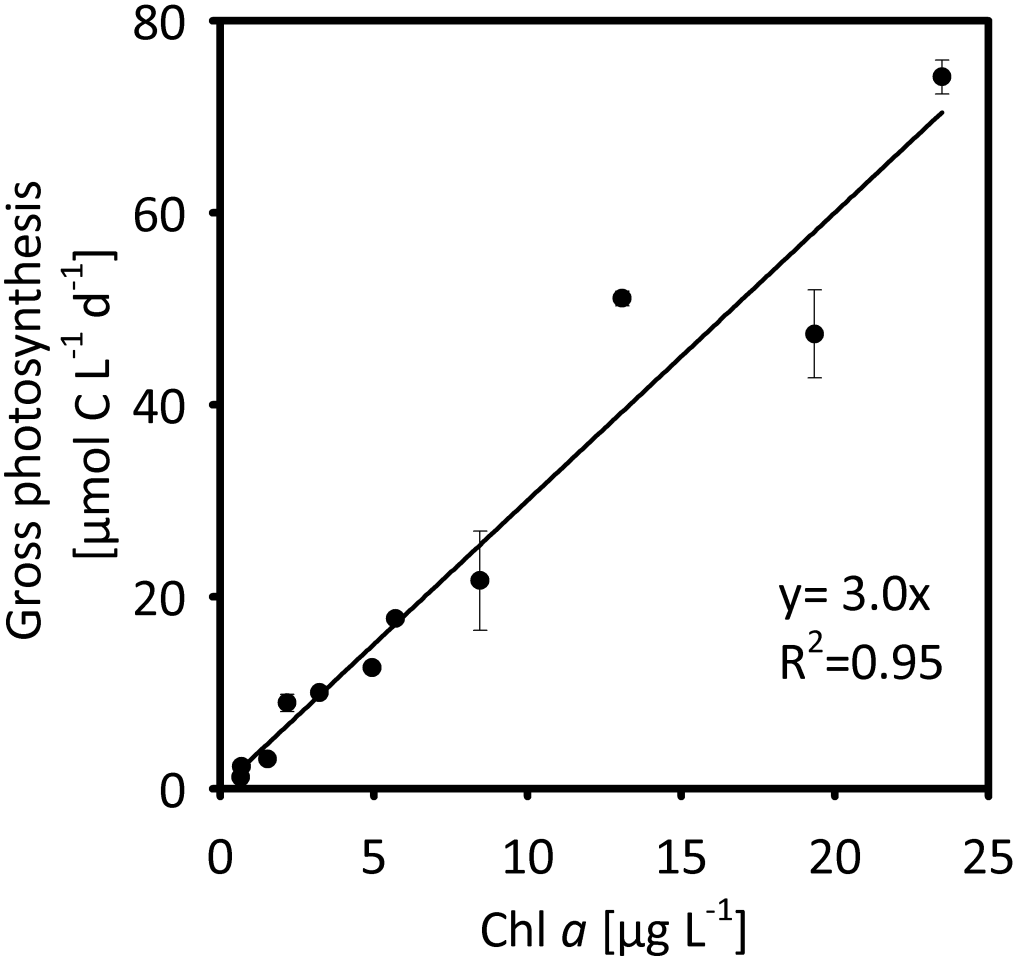
80
60
40
20
0
0
5
10
15
20
25
Gross photosynthesis
[µmol C L-1 d-1]
Chl a [µg L-1]
y= 3.0x
R2=0.95

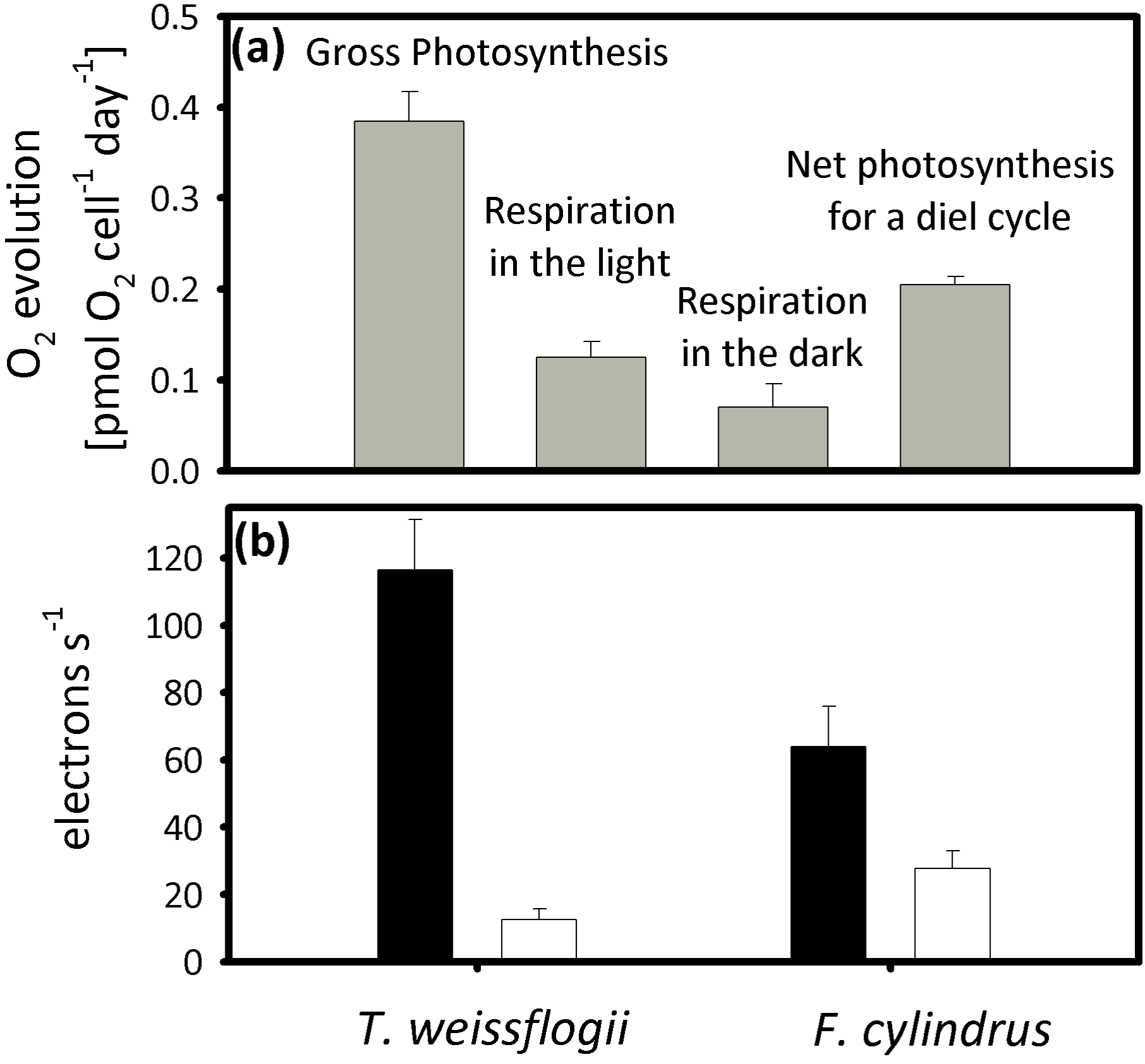
(a) Gross Photosynthesis
Respiration in the light
Net photosynthesis for a diel cycle
Respiration in the dark
O2 evolution [pmol O2 cell-1 day-1]
0.5
0.4
0.3
0.2
0.1
0.0
(b)
electrons s-1
120
100
80
60
40
20
0
T. weissflogii
F. cylindrus